Proceedings of the 2006 IEEE/RSJ
International Conference on Intelligent Robots and Systems
October 9 - 15, 2006, Beijing, China

Haptic Rendering of Biological Elastic Properties based on Biomechanical Characterization

Mehdi Boukallel, Maxime Girot and Stéphane Régnier
Laboratoire de Robotique de Paris
Université Pierre et Marie Curie - Paris 6
CNRS - FRE 2507
18, route du Panorama - BP 61
92265 Fontenay-aux-Roses Cedex, France
{*boukallel, girot, regnier*}*@robot.jussieu.fr*

***Abstract*— This paper deals with the design of a micro-force sensing device for biomechanical characterization of biological samples. This device combines (SPM) techniques and advanced robotics approaches and allows to carry out *in vitro* prolonged observations as well as biomechanical characterization experiments. Elastic properties of biological samples are reflected to the macroscale during the mechanical characterization process by means of a haptic sensing device. Non-linear elasticity theory formalism is used in order to achieve realistic elastic rendering. Mechanical characterization experiments are conducted on human tumoral Epithilial Hella cells in order to demonstrate the efficiency and viability of the proposed system.**

I. Introduction

It is now well established that variety of cells are sensitive to mechanical disturbances from their environment. The response of cells to mechanical inputs is critical in governing cell behavior, not only in cell culture, but also in extension to the physiology of whole organisms as well. This process by which cells convert mechanical stimuli into biochemical signals is called mechanotransduction. Because cells are mechanically coupled to their environment, changes in the extracellular matrix (ECM) or cell mechanics can dramatically change the cell behavior. For example, hepatocytes, mammary epithelial cells, capillary endothelial cells and fibroblasts in culture can be switched from a growth state to a differentiated, non-proliferating state by modifying the stiffness or adhesivity of the ECM. Because of the strong in vitro and in vivo evidence that cell mechanics governs cell behavior, it is not surprising that many different human diseases may arise from abnormalities in the mechanical environment surrounding cells or the ability of cells to properly respond to these forces. For example it is well adopted that tumors are stiffer than normal tissue, as they are frequently detected through physical palpation. In cancer metastasis, tumor cells must dramatically change their physical interactions with surrounding cells and ECM in order to break away, begin migrating, invade blood vessels, extravasate, and grow at distant sites [1]- [3]. This is one of many examples on how cells in a pathological state stop to obey normal biophysical rules, with serious detrimental consequences.

The treatments of many diseases depend in part upon targeting mechanical processes. Understanding cells mechanotransduction will not only provide a more complete understanding of cell behavior, but will also establish new opportunities for increasing the overall efficiency of treatment of pathologies which have a basis in physical perturbations. Thus, the ability to study accurately both mechanical response and their inferences on individual cells is a key component in understanding the complex biological behavior in their environment (growth, development, auto-repair, ...).

Up to date, several robotics and microrobotics experimental setups have been developed to identify the control mechanisms of both individual cell and tissues mechanical responses [4]- [10]. Among these systems, the most promising ones involves Scanning Probe Microscopy (SPM) techniques for nanoscale. The significant research involving AFM make possible the measuring of relevant cells mechanical properties (Young's modulus, bulk modulus, surface roughness, cell adhesion, ...) at the microscale or to investigate cell adhesion and molecules involved in receptor-ligand interactions at the nanoscale [11]- [15]. However, most of these studies have not been performed in biological clean room environment. Since elementary biological functions and mechanical properties of biological cells are widely affected by the experimental conditions, identified properties and behaviors may not be relevant. As the reaction of the biological samples to stress vary greatly in a given lapse time, it is important to monitor the cell response continuously in an *in vitro* environment. Mechanotransduction studies based on AFM techniques are commonly carried out by standard commercial cantilevers with a sharp tip. Some problems can be associated with the use of sharp cantilevers. The nanometers size dimensions of tips can cause important local strains which are higher than elastic domain. Furthermore, depending of the magnitude of the applied force on the soft samples, cantilevers tips as well as the samples can be easily damaged so that the local strain applied in the indented area changes. Since soft organic tissues exhibit very complex mechanical behavior (non-linear, anisotropic, viscoelastic and in some cases also viscoplastic behavior), approaches based on soft contact mechanics are more suitable. This issue has been addressed

1-4244-0259-X/06/$20.00 ©2006 IEEE

in our previous work by using a tipless chemically inert cantilever which is less prone to sharp tip problems [16]. Finally, studies involving AFM techniques for biomedical applications are mainly focused on the accurate determination of the cell mechanical response. Seldom are the studies on mechanotransduction which are extended to *in vitro* tactile sensing of the cell response. Tactile sensing can be a promising solution when combined to traditional biochemical approach to investigate the complex mechanical behavior of cells in their environment and the mechanisms by which biochemical signals are transmitted. Reflect forces as well as physiological changes of cells to the macroscale can lead to a better understanding of the mechanotransduction process. This issue has been addressed in this paper by the developed Force Sensing Bio-Microscope (FSBM) system. This device combines SPM techniques and advanced robotics approaches allowing to carry out *in vitro* prolonged observations on biological samples. A haptic sensing device with 1 DOF is used for investigate either elasticity, elasticity hysteresis or viscoelasticity behaviors. Mechanical characterization experiments are conducted on human tumoral Epithilial Hella cells in order to demonstrate the efficiency and viability of the proposed system.

In the next section, the experimental device produced to perform cell mechanical characterization based on sensing features is presented and detailed in the section II. Section III is devoted to the description of the mechanical modeling of the haptic device. Section IV presents the description of our preliminary experimentation and analysis of cells mechanical characterization using the Force Sensing Bio-Microscope *(FSBM)* under *in vitro* conditions on human tumoral adherent cervix Epithelial Hela cells.

II. Experimental setup overview

The *FSBM* experimental setup provides suitable conditions for study in controlled environment so that the biological cells can be kept several hours in living state by using a cage incubator. Moreover, the mechanical measurement process can be done on the biological sample on an extended lapse of time. Figure 1 shows the overview of the developed *FSBM* device. The *FSBM* is composed mainly with four units: the mechanical sensing unit which performs detection, positioning and sensing features, the imaging/grabbing unit for imaging features, the clean room *in vitro* unit which allows experiments to be conducted in biological environment and the haptic device for the realistic sensing of biological elastic properties. Two computers (master and slave) are used to control the units. The slave computer is assigned to control the mechanical sensing, the imaging and the clean room units while the master computer is dedicated for the haptic device. The slave computer is connected to the master computer using a UDP communication. A user definable interface based on MATLAB® communication toolbox is developed to allows efficient flow communication. The bilateral configuration of the connection between the master and the slave computers is presented in figure 2.

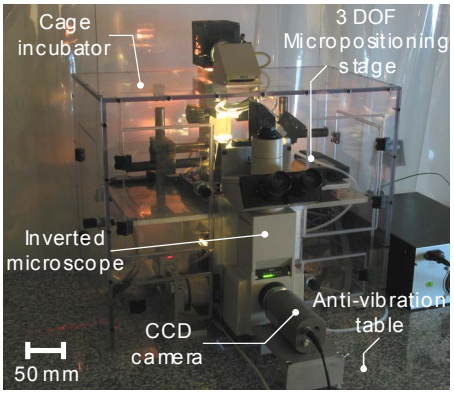

Fig. 1. The *FSBM* experimental setup overview.

A. Mechanical sensing unit

The *FSBM* mechanical sensing unit is based on the detection of the deflection of a cantilever by an optical technique. A four quadrant photodiode with internal amplifiers associated to a low power collimated laser diode (wavelength 650 nm) are used in order to perform both axial and lateral nanoNewtons forces measurements. The total sensing area of the photodiode is 7 mm^2 with a spectral response from 400 to 1100 nm. The optical path of the Gaussian laser beam is optimized using a pair of mirrors and a aspheric condenser glass lens. Hence, a sensitive and accurate detection device is produced for the aim of our study. The sensitivity of the optical detection device is 5 $mV/\mu m$.

A low spring constant (0.2 N/m) uncoated tipless silicon cantilevers is used as probe for the cell mechanical characterization. The lever is 450 μm long, 90 μm large and 2 μm thick. The sample to be studied is accurately positioned below the cantilever by a 3 DOF's (x,y and z) micropositioning encoded stage with a submicrometer resolution (0.1 μm). The kinematic features of the micropositioning stage allows to achieve accurate mechanical measurements in a workspace of 25 x 25 x 25 mm^3 with good repeatability. The configuration

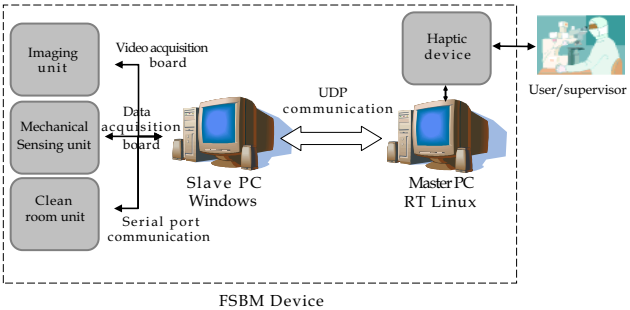

Fig. 2. Block diagram of the *FSBM* device.

of the mechanical sensing unit, including the optical detection device, is presented in figure 3. A magnified picture of the cantilever with the focused laser beam on its reflective surface is shown in the same figure.

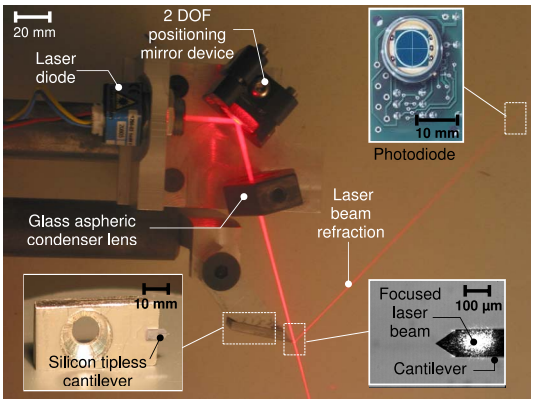

Fig. 3. The mechanical sensing unit.

B. *Imaging/grabbing unit*

The *FSBM* imaging/grabbing unit consists of an inverted microscope (Olympus IMT-2) with Nikon 10x and 20x objectives. A phase contrast device is mounted on the microscope for precise contrast operation. The inverted microscope is fitted out with a CCD camera (754x488 pixels resolution). Using a frame grabber and a specialized imaging PCI (Matrox Imaging) device associated to the CCD camera, automatic mechanical characterization based on image features tracking is achieved.

C. *Clean room* in vitro *unit*

The biological samples need specific requirements to be kept alive outside the *vivo* conditions to carry out prolonged observations. Besides the biological nutrition medium, biological cells need 37 ^oC in temperature and 5% of CO_2 gas. The *FSBM* is equiped with a controlled heating module which maintains temperature on the cage incubator at 37 ^oC using a single thermocouple. The cage incubator ensures a temperature stability within the 0.1 ^oC. A mixed stream composed by a 5% CO_2 and humidified air is fed into a small incubating chamber containing the biological samples, avoiding in this way condensation on the cage walls that could damage the mechanical parts of the microscope and the micropositioning stages. The whole system including the *FSBM* is placed in a negative pressure clean room to protect the biological environment.

D. *Haptic device*

The haptic device consists of Maxon® DC motor coupled with an accurate encoder. The device performs two functions : accurate placement of the cantilever above the sample (z direction) and elastic and visco-elstic haptic rendering. The outstanding technical features of the the DC motor and the components working with allow effective haptic rendering at the macroscale. Besides their compact design, the device presents linear behavior between both the voltage/speed and the load/speed. Since no magnetic detent is used for the motor fabrication, electromagnetic interferences are reduced. Furthermore, the haptic device is able to bear high overload which increase its robustness to bad manipulation. Figure 4 presents the overview of the haptic device. A low mass inertia Aluminum ergonomic disc are fixed to the motor spindle in order to perform efficient manipulation and sensing tasks. The table I summarizes the relevant technical features of the DC motor and the encoder.

TABLE I
HAPTIC DEVICE PARAMETER DATA

Parameter	Numerical value
Maximum current input	2.15 A
Nominal voltage	40 Volts
Inductance resistance	2 Ohms
Maximum torque Γ_m	0.11 Nm
Maximum speed	8200 tr/mn
Angular range	infinite
Angular resolution	1/5000 tr
Efficiency	86 %
Radius of the Aluminum disc	35 mm
Maximum tangential force	2.86 N

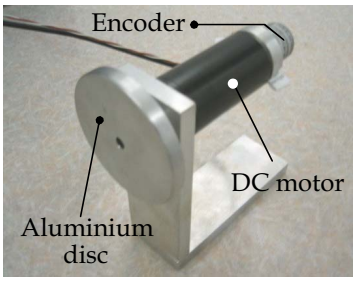

Fig. 4. The haptic device.

III. MECHANICAL MODELING AND CALIBRATION OF THE SENSING DEVICE

In order to perform accurate sensing tasks at the microscale, we have conducted experiment for modeling the mechanical behavior of the haptic device.

A. *Mechanical behavior*

The angular position θ and the speed Ω as a function of the input current I are presented in figure 5(A) and (B) respectively. These curves emphasize the role of the load in decreasing the efficiency of the haptic device but reveal a good linear behavior between speed and current.

Figure 6 shows the load influence on the speed/torque diagram. The torque/speed experimental data are fitted with

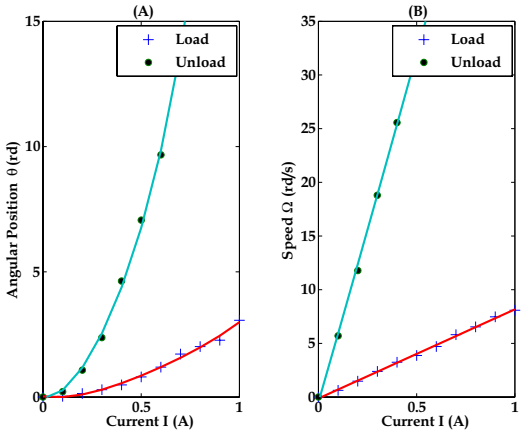

Fig. 5. (A) Angular position θ as a function of the current I. (B) Speed Ω as a function of the current I.

linear interpolation function. The slope of the unload curve is in a good agreement with the manufacturer specifications (Torque constant). The torque Γ_m of the haptic device is measured using a calibrated force cell. One can see that speed decrease linearly with increasing torque for the two cases. Based on this diagram, the identification of the load torque/speed constant is achieved by calculating the slope of the load curve ($K_{torque/speed} = 6.2\ mN.rd^{-1}.s$).

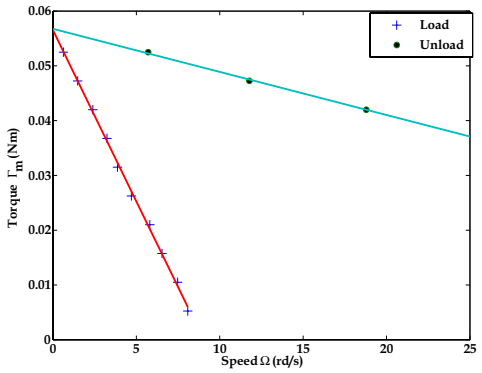

Fig. 6. Influence of the load for the torque/speed behavior.

Figure 7 presents experimental results of hysteresis identification. For this purpose, the encoder output is monitored for an increasing and decreasing values of the input current I during 2 cycles. The sensing device exhibits a weak hysteresis whatever the rotation direction (clockwise and anti-clockwise).

B. Time and frequential response

The haptic device is modeled as a SISO (Single Input, Single Output) system with current I applied to the stator as the input and the speed Ω of the rotor as the output. Since the current-speed obey to linear relationship (cf. figure 7), the resulting model can be considered as an LTI (Linear Time Invariant) system. The step response of the SISO model is presented in figure 8. The time response is fitted with a second order $H(s)$ system as

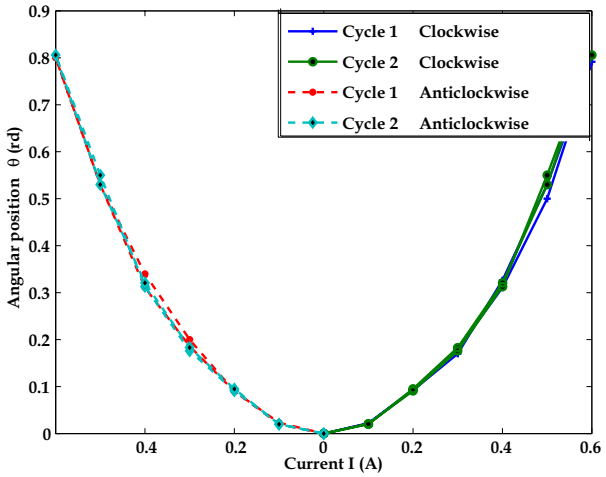

Fig. 7. Hysteresis of the sensing device for clockwise and anti-clockwise rotation.

$$H(s) = \frac{8.09}{0.004s^2 + 0.11s + 1} \quad (1)$$

Figure 8 reveals obviously the adequacy between the modeled and the measured time response behavior of the haptic device. Both measured and modeled frequential responses of the sensing device are presented in figure 9 by means of the bode diagram. The fitted model simulate appropriately the frequential behavior of the haptic device.

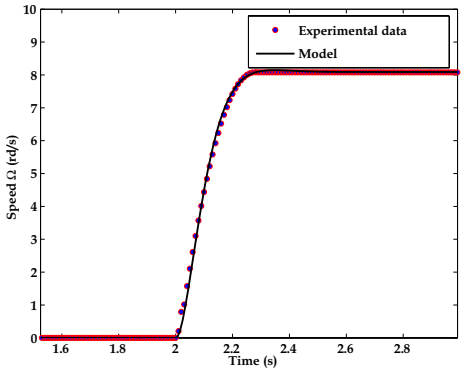

Fig. 8. Step response of the SISO model.

C. Non-linear Adaptative Spring (NAS) for elastic and elastic hysteresis sensing

Since the mechanical response of soft elastic material (load/deformation) does not obey to linear relationship (Hooke's law), they can be modeled as a non-linear spring. A typical load-elongation diagram for soft tissue is shown in figure 10. We can note that loading and unloading occur on different load-deformation paths. As this diagram can be segmented to linear areas, the mechanical behavior can be modeled as n serial linear springs with spring constants $K_1,\ K_2,\ ...,\ K_n$.

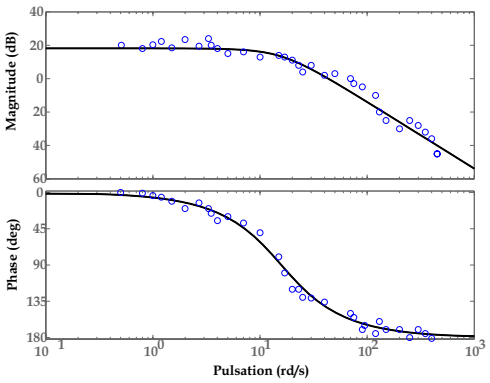

Fig. 9. Bode diagram of the SISO model.

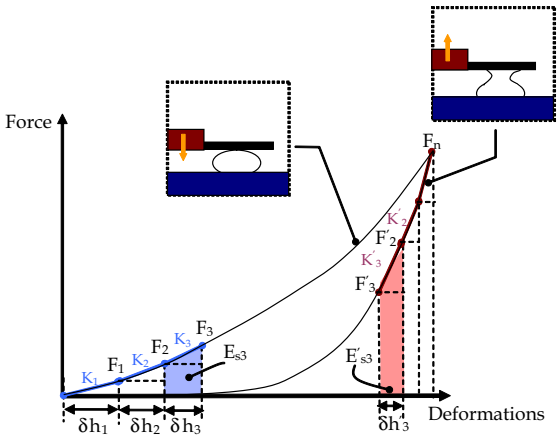

Fig. 10. A typical load-elongation diagram for soft tissue.

During the load path, the strain energy E_{si} stored by each linear spring is expressed as the area below the curve and calculated as

For i=1

$$E_{s1} = E_1 = \frac{1}{2}K_1\delta h_1^2 \tag{2}$$

Where δh_1 is the deformation resulting for the applied variation load δF_1

For i=2

$$E_{s2} = \frac{1}{2}K_2\delta h_2^2 + \delta h_2 F_1 \tag{3}$$

For i=3

$$E_{s3} = \frac{1}{2}K_3\delta h_3^2 + \delta h_3 F_2 \tag{4}$$

For i=n

$$E_{sn} = \frac{1}{2}K_n\delta h_n^2 + \delta h_n F_{n-1} \tag{5}$$

Then, the total strain energy E_{Ti} stored by the non-linear spring for a given deformation δh_i is the sum of energies stored by each linear springs as

For i=1

$$E_{Ti} = E_{s1} = \frac{1}{2}K_1\delta h_1^2 \tag{6}$$

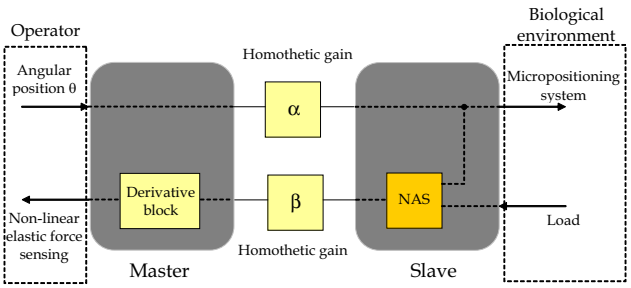

Fig. 11. Overview of the Master/Slave bilateral coupling scheme.

For i=2

$$E_{T2} = E_{s2} + E_{s1} = \frac{1}{2}K_1\delta h_1^2 + \frac{1}{2}K_2\delta h_2^2 + \delta h_2 F_1 \tag{7}$$

For i=3

$$E_{T3} = E_{s3} + E_{s2} + E_{s1} = \frac{1}{2}K_1\delta h_1^2 + \frac{1}{2}\delta h_2(K_2\delta h_2 + 2F_1) + \frac{1}{2}\delta h_3(K_3\delta h_3 + 2F_2) \tag{8}$$

For i=n

$$E_{Tn} = \frac{1}{2}K_1\delta h_1^2 + \frac{1}{2}\sum_{2}^{n}(\delta h_i(K_i\delta h_i + 2F_{i-1})) \tag{9}$$

As energy formulas are discretized, software implementation becomes easier. Strain energy equations and their iterative calculations are implemented in the slave computer based on Matlab® Simulink Toolbox. Figure 11 shows the overview of the adopted Master/Slave bilateral coupling scheme. The homothetic gains α and β are determined during the calibration process. The appropriate values of the homothetic gains in our case are $\alpha = 5\ 10^{-4}\ \mu m/rd$ and $\beta = 1500\ N/J$.

For the unload path the same approach is adopted. If we note $K_i^{'}$ and $\delta h_i^{'}$ the ith constant spring and the sample deformation, thus, the total strain energy $E_{Ti}^{'}$ is expressed as

$$E_{Tn}^{'} = \frac{1}{2}K_1^{'}\delta h_1^{'2} + \frac{1}{2}\sum_{2}^{n}\left(\delta h_i^{'}(K_i^{'}\delta h_i^{'} + 2F_{i-1}^{'})\right) \tag{10}$$

IV. Experimentations

Haptic sensing experimentations are conducted on human tumoral Epithilial Hella cell (EpH). The cells are chosen since they are adherent and present an interesting soft elastic behavior. The *EpH* cells can be assimilated morphologically to elliptical cells with a thin surrounding biomembrane. In the present study, the average dimensions of the biological sample is 10 μm long, 9 μm large and 6 μm height (cf. figure 12).The Epithelial Hela cells *(EpH)* are prepared on Petri dishes with specific culture medium formed by Dulbecco's Modified Eagle's Medium (DMEM) with high glucose and L-glutamine components and 10 % of foetal bovine serum.

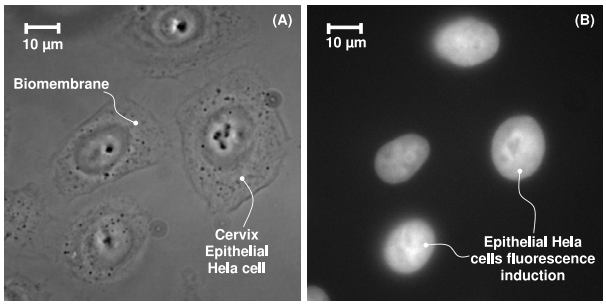

Fig. 12. (A) Magnified image of the cervix Epithelial Hela cells obtained with an 63x objective. (B) The cervix Epithelial Hela cells morphology observed by fluorescence techniques.

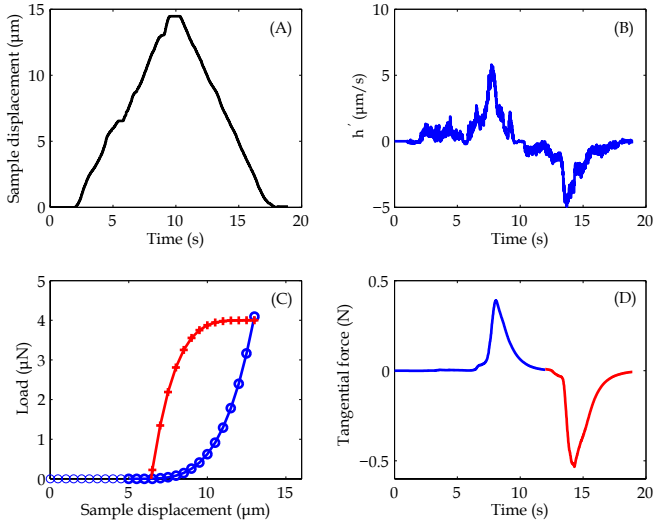

Fig. 13. (A) Biological sample displacement carried out by a human operator interface. (B) Derivative form of the sample deformation as function of time experiment. (C) Elastic behavior of the *EpH* cells. (D) Tangential forces sensed by the human operator.

Figure 13(A) shows the biological sample displacement carried out by a human operator using the haptic device. Displacements less than 15 μm are achieved during this experiment. The cell deformation δh is monitored by calculating the difference between the vertical position of the sample and the cantilever deflection. Figure 13(B) shows the derivative form of the sample deformation $\dot{h}$ as function of time experiment. According to this figure, the studied biological sample exhibits the same deformation amplitude whatever the load-deformation path (load and unload). Figure 13(C) reveals the elastic behavior of the biological sample as well as the elastic hysteresis. This curve is obtained using the discretized strain energy formulas presented in the last section. In opposition to the sample deformation diagram (cf. figure 13(B)), this figure emphasize the difference between the load and unload paths. Since the elastic behavior of the biological sample is disymmetric, the operator senses different amplitude forces for the load and unload paths. Hence, the forces sensed are more important in the case of the unload path since the gradient of the stored strain energy is bigger.

V. Conclusion

This paper has presented the development of a microforce sensing system for *in vitro* mechanical cell characterization. The experimental setup combines Scanning Probe Microscopy (SPM) techniques with advanced robotics approaches. Mechanical characterization is conducted using the *FSBM* on tumoral human Epithelial Hela adherent cells. These experiments demonstrate the efficiency of the experimental setup developed to explore the non-linear elastic properties of adherent biological samples. Non-linear elasticity theory formalism is used in order to achieve realistic elastic rendering for the macroscale.

References

[1] D.-E. Ingber, "Cancer as a disease of epithelial-mesenchymal interactions and extracellular matrix regulation".Differentiation, vol. 70, pp. 547-560, 2002.

[2] C.-S. Chen, M. Mrksich, S. Huang, G.-M. Whitesides, D.-E. Ingber, "Geometric control of cell life and death". Science, vol. 276, pp. 1425-1428, 1997.

[3] C.-M. Lo, H.-B, Wang, M.Dembo, Y.-L. Wang, "Cell movement is guided by the rigidity of the substrate", Biophys J., vol. 79, pp. 1957-1964, 2000.

[4] Y. Sun and B.-J. Nelson, "MEMS for cellular force measurements and molecular detection", Journal of Information Acquisition, vol. 1, no. 1, pp. 23-32, January 2004.

[5] K.-J. Van Vliet, G. Bao and S. Suresh, "The biomechanics toolbox: experimental approaches for living cells and biomolecules", Acta Materialia Journal, vol. 51, pp. 5881-5905, August 2003.

[6] D.-H. Kim, S. Yun and B. Kim, "Mechanical force response of single living cells using a microrobotic system", in proceedings of the Int. Conference on Robotics and Automation, pp. 5013-5018, 2004.

[7] J. Guck, R. Ananthakrishnan, C.-C. Cunningham and J. Kas, "Stretching biological cells with light", J.Physics:Condens. Matter, vol. 14, pp. 4843-4856, May 2002.

[8] J.-M. Sharp, A.-R. Clapp and R.-B. Dickinson, "Measurement of long-range forces on a single yeast cell using a gradient optical trap and evanescent wave light scattering", Colloids and Surface B:Biointerfaces, vol. 27, pp. 355-364, 2003.

[9] D.-G. Grier, "A revolution in optical manipulation", Nature, vol. 424, pp. 810-816, 2003.

[10] M. Lukkari and P. Kallio, "Multi-purpose impedance-based measurement system to automate microinjection of adherent cells", in proceedings of the Int. Sympos. on Computational Intelligence in Robotics and Automation", pp. 20-26, 2005.

[11] M. Radmacher, "Measuring the elastic properties of biological samples with AFM", IEEE Engineering in Medicine and Biology, pp. 47-57, 1997.

[12] O. Sahin, G. Yaralioglu, R. Grow, S. -F. Zappe, A. Atalar, C. Quate and O. Solgaard, "High-resolution imaging of elastic properties using harmonic cantilevers", Sensors and Actuators A, vol. 114, pp. 183-190, February 2004.

[13] S. Park, K. Costa and G. Ateshian, "Microscale frictional response of bovine articular cartilage from atomic force microscopy", Journal of Biomechanics, vol. 37, 1687-1697, February 2004.

[14] E.-K. Dimitriadis, F. Horkay, J. Maresca, B. Kachar and R.-S. Chadwick, "Determination of elastic moduli of thin layers of soft material using the atomic force microscope", Biophysical Journal, vol. 82, pp. 2798-2810, May 2002.

[15] X. Yao, J. Walter, S. Burke, S. Stewart, M.-h. Jericho, D. Pink, R. Hunter and T.-J. Beveridge, "Atomic force microscopy and theoretical considerations of surface properties and turgor pressures of bacteria", Colloids and Surfaces B: Biointerfaces, vol. 23, pp. 213-230, May 2002.

[16] M. Boukallel, M. Girot, S. Régnier, "Enhanced near field force probing for mechanical cell characterization", in proceedings of the IEEE/RAS-EMBS International Conference on Biomedical Robotics and Biomechatronics (BioRob), February 2006.